Acta Cryst. (1956). 9, 479

The Measurement of Growth and Deformation Faulting in Hexagonal Cobalt

By T. R. Anantharaman and J. W. Christian

The Inorganic Chemistry Laboratory, Oxford, England

(*Received* 11 *January* 1956)

The use of Fourier and line-breadth methods for the determination of stacking-fault parameters in hexagonal close-packed metals has been investigated. Greatest accuracy is probably obtained by Fourier analysis of the $\{10\bar{1}1\}$ line, but analyses of other lines are required in addition when more than one type of faulting is present. Line-breadth methods usually give satisfactory results, and are valuable in determining the predominant type of faulting. Spontaneously transformed cobalt powders often contain mainly growth faults, whereas specimens which have been deformed to complete the martensitic transformation contain mainly deformation faults. Specimens with mixed faulting have also been obtained; an alternative hypothesis, that the faults are 'clustered', will explain the line-breadth results, but not those obtained by Fourier analysis.

1. Introduction

Powder specimens of cobalt give anomalous X-ray diffraction patterns because of the presence of stacking faults in the h.c.p. phase (Edwards & Lipson, 1942; Wilson, 1942, 1949). The general theory of diffraction from layer structures containing random mistakes is now well understood (Wilson, 1949; Jagodzinski, 1949; Gevers, 1953), and detailed expressions for the diffracted intensity have been obtained for most kinds of fault. Wilson's theory considered only growth faults, but Paterson (1952) extended it to deformation faults in f.c.c. structures, and later papers have dealt with h.c.p. deformation faults (Christian, 1954) and co-existing growth and deformation faults (Gevers, 1954). The effects of the more complex 'extrinsic' faults (Frank & Nicholas, 1953) have not been considered in detail, but these may have higher energies, and so be less frequent. They are neglected in the present paper.

Faulting in f.c.c. materials produces displacements in the positions of some of the diffraction peaks, and this provides a convenient measure of the amount of faulting. In h.c.p. structures, the peak position does not change, and measurements of line breadth or line shape have to be made. In recent years, considerable attention has been paid to the interpretation of broadened Debye–Scherrer lines in terms of mean square atomic displacements (strain coefficients) and particle-size effects. There appears, however, to have been no quantitative work on fault broadening in cobalt since the original paper by Edwards & Lipson.

In the course of experiments on the factors affecting growth and deformation faulting in cobalt, we experienced difficulty in obtaining reproducible results from different lines on the same photograph. Similar discrepancies are evident when the data of Edwards & Lipson are examined. The present paper describes the result of an investigation into the accuracy of the various possible methods of determining the faulting parameter in h.c.p. materials. The methods tried have naturally been suggested by the many thorough investigations into strain and particle-size broadening.

2. Experimental methods

Hydrogen-reduced cobalt powder (99·98% pure), of 250–300 mesh, was used in all the experiments. After annealing *in vacuo* for one day at either 500 or 800° C., Debye–Scherrer specimens were prepared by lightly rolling into rods with dilute Canada balsam solution. This procedure imparted very mild stresses to the specimens, and had the advantage of producing variations in the proportion of the h.c.p. phase and the degree of faulting. A few specimens were annealed, cooled and photographed in thin-walled silica capillaries, thus minimizing all stresses. X-ray photographs were taken in 9 or 19 cm. diameter cameras, using crystal monochromatized or (occasionally) filtered radiation from cobalt, nickel or molybdenum targets; monochromatized nickel radiation was used for most of the work. The films were photometered by hand, using a direct-reading instrument and taking readings every 0·02 mm. The exposures were regulated to ensure that the photometered regions always came within the linear portion of the film blackening X-ray intensity relation; this region was found by means of a calibrated step wedge. Greater accuracy would probably have been obtained by the use of Geiger counter equipment, but this was not available when the work was started.

The $K\alpha_1$ portion of a composite $\alpha_1-\alpha_2$ doublet was obtained from the observed photometer trace by a graphical procedure (Rachinger, 1948), and an analytical version of the method (Anantharaman & Christian, 1953) was used to assist in obtaining self-consistent background levels. The α_1 components were always found to be symmetrical about their peaks, as required by theory.

3. Methods of calculation

The diffraction theory is based on the assumption that the faults are distributed at random and occupy whole planes. The parameters α, α' are the probabilities of finding a growth or a deformation fault at any plane, and, to a first approximation at least, may be regarded as the fractional areas of the two kinds of fault on all atomic close-packed planes in the more realistic case where the faults do not occupy whole planes. We use normal hexagonal indices ($HK.L$), and we let h_3 be a continuous variable in the c^* direction of reciprocal space. For broadened lines, $H-K = 3N\pm 1$ (N any integer) and the diffraction effects depend on whether L is even or odd. The intensity distribution in reciprocal space, $\beta(\xi)$, is a function of the displacement $\xi = h_3 - L$ from the nearest diffraction maximum (reciprocal-lattice point), and we suppose this has integral breadth β and integrated intensity T. The last two quantities are defined between limits $\xi = \pm 1$. In terms of a parameter, ϱ, defined below, the results may now be conveniently summarized in the equations:

$$\beta(\xi) = \frac{T}{2}\left[1+2\sum_{m=1}^{\infty}\varrho^m \cos \pi m\xi\right] \tag{1a}$$

$$= \frac{T}{2}\cdot\frac{1-\varrho^2}{1-2\varrho\cos\pi\xi+\varrho^2}\,, \tag{1b}$$

$$\beta = 2(1-\varrho)/(1+\varrho)\,. \tag{2}$$

The values of ϱ to be used in equations (1) and (2) are $\varrho = \varrho_e$, $\varrho = -\varrho_o$ for values of L which are even and odd respectively, where

$$\left.\begin{aligned}\varrho_e &= \tfrac{1}{2}\{-\alpha+[\alpha^2+(4-8\alpha)(1-3\gamma)]^{\frac{1}{2}}\}\,,\\ \varrho_o &= \tfrac{1}{2}\{-\alpha-[\alpha^2+(4-8\alpha)(1-3\gamma)]^{\frac{1}{2}}\}\,,\end{aligned}\right\} \tag{3}$$

and

$$\gamma = \alpha'(1-\alpha')\,.$$

The general expressions for ϱ_e and ϱ_o are due to Gevers (1954); it is readily verified that they reduce to those for pure growth and deformation faulting if α, α' are respectively equated to zero. If faulting is predominantly of one kind, this is shown by the relation between the breadths of the lines with L even and odd. For growth faults only, $\beta_e/\beta_o = 3$, whilst for deformation faults only, $\beta_e/\beta_o = 1$.

The integrated intensities, T, for L even and odd are given by the relations

$$T_e = C(1+2\varrho_o)/(\varrho_o-\varrho_e)\,,\quad T_o = C(1+2\varrho_e)/(\varrho_e-\varrho_o)\,, \tag{4}$$

where C is a constant.

In principle, the values of α, α' may be calculated from experimental results using any of the equations (1), (2) or (4). The predicted intensity distributions in reciprocal space may be compared with those measured from single-crystal photographs, but in practice the partially averaged effects obtained in powder photographs have to be used for quantitative work. It is often possible to produce heavy faulting only in powder specimens.

If $B(x)$ is the observed profile of a broadened line, where x is a linear dimension along the film, and $b(x)$ is the corresponding profile in the absence of faults, then, as first shown by Jones (1938), we have

$$B(x) = \int_{-\infty}^{\infty} b(x)\beta(x-z)\,dz\,, \tag{5}$$

where $\beta(x)$ is the diffraction profile (suitably normalized), and is simply related to $\beta(\xi)$. The main difficulties in interpretation arise because it is not possible to obtain $B(x)$ accurately between limits of x corresponding to $\xi = \pm 1$. Between limits $x = \pm x_B$, only part of the intensity will be recorded, and the background level will be incorrectly measured. The observed distribution will be

$$\left.\begin{aligned}B_{(x_B)}(x) &= B(x)-B(x_B)\,, \quad |x| < |x_B|\,,\\ B_{(x_B)}(x) &= 0\,, \quad |x| > |x_B|\,.\end{aligned}\right\} \tag{6}$$

The difficulty was recognized by Wilson (1942), who assumed that photometering between limits $x = \pm x_B$ is equivalent to measuring the intensity in reciprocal space between limits $\xi = \pm\nu$. He thus derived the following equations for the observed integrated intensity and integral breadth in reciprocal space:

$$T_{(\nu)} = T\left[\frac{2}{\pi}\arctan\frac{1+\varrho}{1-\varrho}\tan\frac{\pi\nu}{2} - \frac{(1-\varrho^2)\nu}{1-2\varrho\cos\pi\nu+\varrho^2}\right], \tag{7}$$

$$\beta_{(\nu)} = 2\frac{T_{(\nu)}}{T}\cdot\frac{1}{\left(\dfrac{1+\varrho}{1-\varrho}-\dfrac{1-\varrho^2}{1-2\varrho\cos\pi\nu+\varrho^2}\right)}\,. \tag{8}$$

If faulting of one kind only is present, the measurement of α requires the determination of the two experimental quantities $\beta_{(\nu)}$ and ν from any broadened line. If both kinds of fault are present, measurements must be made on at least two lines, having L even and odd respectively. The method has obvious disadvantages, however, and it may be objected in particular that the measured function $B_{(x_B)}(x)$ is not strictly related to a function $\beta_{(\nu)}(\xi)$ by an equation of type (5).

A more direct method of measuring ϱ, and hence α, is suggested by equation (1a), which expresses the intensity $\beta(\xi)$ as a Fourier series. The procedure described by Stokes (1948) for separating the diffraction and instrumental broadening factors enables the coefficients of this series to be found. It is also possible, in principle, to determine α from the quantities $T_{(\nu)}$ and ν, but this is unlikely to give accurate results.

4. Use of Fourier methods

Equation (1) shows that $\beta(\xi)$ is a periodic function of ξ for both odd and even lines. To obtain the true values of the Fourier coefficients, $A_n^{\beta} = \varrho^n$, we have

thus to divide the regions of x corresponding to the full period into $2s$ divisions of equal ξ, and perform summations of the type

$$A_n^B = \sum_{r=-s}^{s} B(x_r)\cos(\pi rn/s)\,, \quad A_n^b = \sum_{r=-s}^{s} b(x_r)\cos(\pi rn/s)\,.$$

Beevers–Lipson strips are unsuitable for this purpose, since dividing the whole period into only 60 or 120 divisions gives an insufficient number of values on the measurable parts of the lines. A value of $s = 200$ was found convenient for the $\{10\bar{1}1\}$ line, giving intervals of $\sim 0{\cdot}1$ mm. in x on 9 cm. photographs with nickel radiation. Tables of $\cos 2\pi nh$ were therefore prepared at intervals of 0·005 in h and for values of $n = 1$–10, 15, 20, 25, 30, 40 and 50. As explained above, the $K\alpha_2$ components of the lines were eliminated graphically before making the Fourier summations; this procedure was much simpler than the alternative of eliminating $K\alpha_2$ during the summations, and tables of sines were not needed.

Since faulting cannot be readily removed, the profile $b(x)$ must be obtained from a neighbouring standard line. This restricts the method to those broad lines which have well separated sharp lines as close neighbours. In principle, curves of the Fourier coefficients of the sharp lines as a function of deviation angle could be plotted, as is done for the breadths, thus giving the shape of the apparatus function at all angles. However, this procedure would be very tedious and unreliable. In the present work, we have found that the Fourier method can only be readily applied to the $\{10\bar{1}1\}$ line.

For normal amounts of faulting, the Fourier coefficients of $\beta(x)$ decrease very slowly with n. This means that high accuracy cannot be expected, especially for higher values of n, since the coefficients of $B(x)$ do not decrease sufficiently rapidly compared with those of $b(x)$. This disadvantage, of course, appears in all methods of measuring the faulting parameter; it means, for example, that the breadth of $B(x)$ is not very much greater than that of $b(x)$.

The diffraction shape $\beta(x)$ has a very long 'tail'. The parts of a line which are not photometered will thus lead to considerable errors in the values of A_n for small n, as pointed out by Eastabrook & Wilson (1952). An investigation of this effect for strain broadening has been made by Williamson & Smallman (1954); in order to test its importance in the present work, we have followed the procedure of these latter workers and carried out a numerical analysis on a theoretical line shape. The results are shown in Table 1. We assumed $\alpha = 0{\cdot}090$, and the calculated intensity values from equation (1*b*) for an odd line were rounded to the nearest 1% of the peak intensity. Three sets of values are given, the background level being assumed to have its correct value, and to be placed too high by 1 and 2% respectively of the peak intensity. In the latter two cases, the parts of the line actually recorded correspond to $\frac{1}{8}$th and $\frac{1}{12}$th of the whole period, and

Table 1. *Fourier coefficients derived from numerical analysis of theoretical line with* $\alpha = 0{\cdot}090$.

n	$A_n=(-\varrho_0)^n$	A_n^1; normal background	A_n^1; background 1% high	A_n^1; background 2% high
0	1·000	0·932	0·866	0·816
1	0·952	0·932	0·866	0·816
2	0·906	0·928	0·866	0·816
3	0·862	0·872	0·834	0·784
4	0·820	0·832	0·822	0·768
5	0·780	0·784	0·770	0·752
6	0·743	0·744	0·738	0·728
7	0·707	0·700	0·702	0·700
8	0·673	0·656	0·670	0·672
9	0·641	0·624	0·638	0·640
10	0·609	0·592	0·606	0·616
15	0·475	0·468	0·462	0·460
20	0·370	0·364	0·374	0·368
25	0·289	0·288	0·282	0·284
30	0·225	0·228	0·226	0·228
40	0·137	0·132	0·142	0·128
50	0·083	0·096	0·090	0·088

it is seen from the table that the calculated A_n^β values correspond to the theoretical values for $n > 4$ and $n > 6$ respectively.

In an actual experiment, the A_n^β values are multiplied by an unknown constant, and it is usual to normalize to $A_0^\beta = 1$. If we call these normalized values A_n', we have:

$$A_n' = \Delta_n \varrho^n / \Delta_0\,,$$

where Δ_n is a function of n and represents the tail errors. As n increases, the tail errors become unimportant, and $\Delta_n \to 1$. A graph of $\log A_n'$ against n should thus be curved at first, but should soon become a straight line of slope ϱ. From this slope, α may then be determined.

In Fig. 1(*a*) we show an experimental $\log A_n'$ versus n plot for a $\{10\bar{1}1\}$ line from a specimen containing growth stacking faults. The profile $b(x)$ was obtained from the neighbouring $\{200\}$ cubic line, which is of comparable intensity. The graph is a straight line of slope $-0{\cdot}022$ from $n = 3$ to $n = 20$. From the relation between the breadths of the odd and even lines, it was obvious that faulting was predominantly of the growth type, and the value of α thus obtained (0·092) agreed well with estimates based on line-breadth measurements.

The results shown in Fig. 1(*a*) are not quite typical; they represent one of the best $\log A_n'$ versus n curves that we have obtained. In a large number of cases, curves of the type shown in Fig. 1(*b*) were obtained. The first part of the curve has the expected shape, and there is a short straight-line region from which a value of α may be deduced, but at higher values of n (ranging from 9 to 20 in different films) the curve flattens and then gives rise to an oscillating portion. These effects are almost certainly due partly to the decrease in accuracy in determining A_n' for large n, referred to above, although the flattening may also be caused by other effects (see below).

Fig. 1(*b*) includes the Fourier plots from two odd lines, $\{10\bar{1}1\}$ and $\{20\bar{2}1\}$, and the slopes of the straight-line portions are in good agreement with each other. Attempts were made to obtain Fourier plots from the $\{10\bar{1}2\}$ and $\{10\bar{1}3\}$ lines on the same film, but the profiles were too uncertain for very reliable results. The curve for the $\{10\bar{1}2\}$ line also has a short linear portion, and is shown in Fig. 1(*c*). Values of α obtained from Figs. 1(*b*) and (*c*) on the assumption of random growth faulting are $\sim 0{\cdot}080$ and $\sim 0{\cdot}043$ respectively, and this assumption is thus shown to be incorrect unless the errors are larger than anticipated. A similar discrepancy between odd and even lines was found in this and other films by the line-breadth method, and suggests either that there is some deformation faulting present, or that the diffraction theory is inadequate in some way.

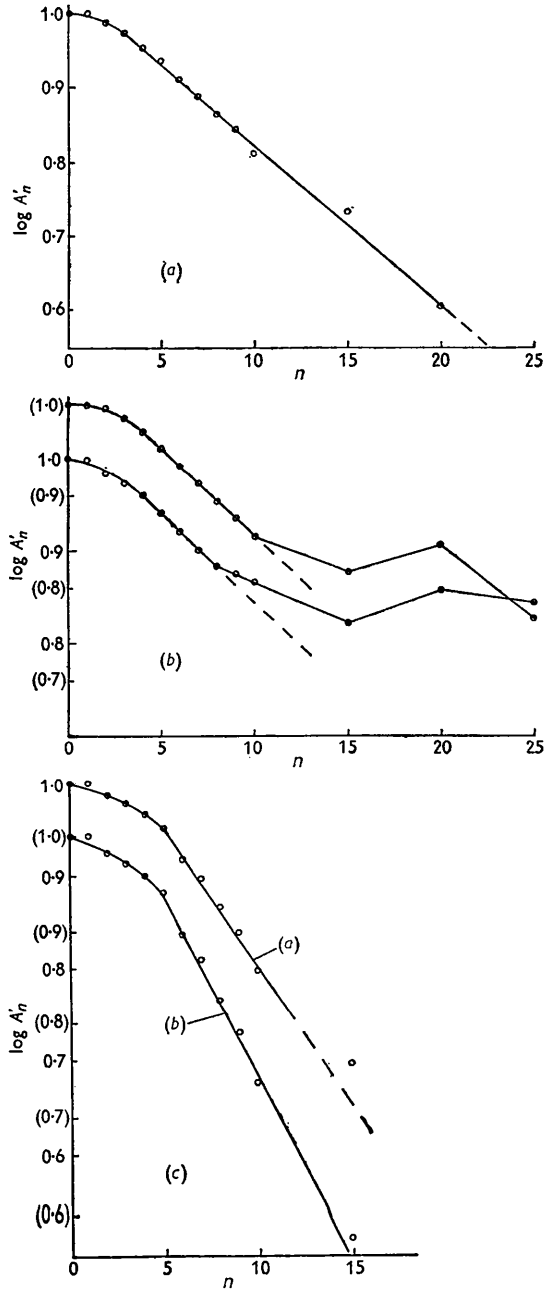

Fig. 1. (*a*) Fourier plot of $\{10\bar{1}1\}$ line for specimen containing growth faults.
(*b*) Fourier plots of $\{10\bar{1}1\}$ and $\{20\bar{2}1\}$ lines. Ordinate scales displaced for clarity; bracketed values are for $\{20\bar{2}1\}$.
(*c*) Fourier plot of $\{10\bar{1}2\}$ line from the same film as the results in Fig. 1(*b*). Curve (*a*): assuming random faulting; curve (*b*): assuming 20% of the diffracting volume is unfaulted. A'_n values for curve (*b*) are re-normalized to $A'_0 = 1$, but ordinate scales are displaced for clarity.

Calculation of α and α' from the slopes of the curves by means of equation (3) leads to the values $\alpha = 0{\cdot}024$, $\alpha' = 0{\cdot}022$, which seem quite reasonable. However, the line-breadth results suggested the possibility of an alternative explanation, namely that the faults are clustered rather than randomly distributed. To a first approximation, a specimen containing clustered faults may be treated as a mixture of randomly faulted and unfaulted regions, and we assume that the diffraction effects are additive. The $\log A'_n$ versus n curve calculated on the basis of random faulting would thus tend to a constant minimum value with increasing n, instead of to zero, and the curves of Figs. 1(*b*) and (*c*) do show evidence of such a tendency. To obtain the Fourier coefficients of the faulting, we have now to subtract constant amounts from the measured coefficients. Fig. 1(*c*) also shows the $\log A'_n$ versus n plot for the $\{10\bar{1}2\}$ line, assuming that 20% of the diffracting volume is unfaulted, and that the faults are randomly distributed in the remainder. The straight-line region now extends to rather higher n values, and the change in slope increases the value of α (assuming growth faults only) to $\sim 0{\cdot}06$. The value of α from the odd lines is also increased, though to a smaller extent, so that the quantitative disagreement has been reduced but not eliminated. The discrepancy could be caused by the rather unrealistic assumption about the diffraction effects of clustered faults, but it seems more probable that the correct explanation lies

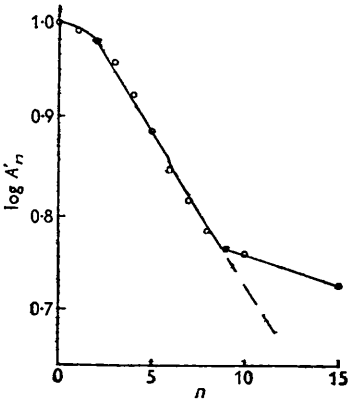

Fig. 2. Fourier plot of $\{10\bar{1}1\}$ line for specimen containing deformation faults.

in the presence of both kinds of fault, rather than in the clustering of growth faults alone. We hope to pursue this question further with more accurate Geiger counter data; in the meantime the present results suggest that accurate values of ϱ may be obtained from the Fourier plot of the $\{10\bar{1}1\}$ line, but the type of faulting and the possible existence of other effects must be checked by line-breadth and/or line-shape measurements on the remaining lines.

Cobalt powder which was mechanically deformed in order to complete the transformation was found to contain faults which were predominantly of the deformation type. The lines with $L = 0$ or $H-K = 3N$ were still sharp, but the other lines were broadened by approximately equal amounts. Fig. 2 shows the Fourier plot of the $\{10\bar{1}1\}$ line from such a film; the straight-line portion gives $\alpha' = 0{\cdot}051$.

5. Use of line-breadth measurements

The calculation of α from the observed profiles $B(x)$ and $b(x)$ by measurement of line breadths will be discussed in this section. The calculations required are not so tedious as those in the previous section, and the method has the advantage of being more readily applicable to all the lines on a powder photograph. The stages in the calculation may be enumerated as follows:

(1) Measurement of the breadth, B_x, of $B(x)$ and of the corresponding standard breadth b_x.

(2) Calculation of the diffraction breadth, β_x, and hence of $\beta_{(\nu)}$ in equation (8).

(3) Calculation of ν from the measured limits of x.

The measurement of B_x requires little comment, except to point out the difficulties of locating the background level with diffuse high-angle lines (e.g. $\{20\bar{2}2\}$ and $\{20\bar{2}3\}$ with nickel radiation). The integral breadths of these lines were never considered reliable.

Since faults cannot be removed by annealing, b_x cannot be measured directly, and a curve of standard breadths versus deviation angle must be plotted. Edwards & Lipson used the sharp lines from f.c.c. cobalt for this purpose, and, in addition, the h.c.p. lines with $L = 0$ are almost unbroadened in powder photographs and may also be used as standards. With nickel radiation, this gives only three lines which may be used freely, namely $\{10\bar{1}0\}$, $\{200\}$ and $\{400\}$. It was found possible to separate $\{222\}$ from its interfering neighbour $\{0004\}$ merely by finding the correct background level, using equations equivalent to (5) and (6) of Anantharaman & Christian (1953). Three other pairs $\{111\}$ and $\{0002\}$, $\{220\}$ and $\{11\bar{2}0\}$, and $\{311\}$ and $\{11\bar{2}2\}$ were separated by a slightly generalized version of the method for doublet separation.

The relation between β_x, b_x and B_x depends on the profiles of the lines. When Stokes' method is used, β_x is obtained directly, but the object of the line-breadth method is to find a functional relation between the three quantities which will obviate the need for calculating the Fourier coefficients. In simple cases, equation (5) may be solved directly to give this relation, either by fitting $B(x)$ and $b(x)$ to analytical expressions, or by assuming an expression for $\beta(x)$ from the diffraction theory, together with an analytical form for $b(x)$.

In our results, we observed that none of the analytical line profiles used by previous workers were very good approximations to $B(x)$ and $b(x)$. The best fit for both profiles was obtained from expressions of the form $C/(1+k^2x^2)^2$ which are intermediate between Gaussian and Cauchy line shapes. The relation between the breadths when both are of this form has been found by Schoening, Niekerk & Haul (1952). It seemed worth while also, however, to derive the relation which is valid if $b(x)$ only is assumed to have this shape, and $\beta(x)$ is given its correct shape as indicated by the diffraction theory. In an Appendix, we show that this relation is given by:

$$\beta_x/B_x = \tfrac{1}{2}\{1-4(b_x/B_x)+[8(b_x/B_x)+1]^{\frac{1}{2}}\} . \qquad (9)$$

In Fig. 3, we show the various relations between the three breadths, plotted in the usual form of b/B against β/B, which have been used by different workers. The extreme curves of Scherrer (1920) and Warren (1941) do not seem to correspond to conditions encountered in practice. The curve of equation (9) is

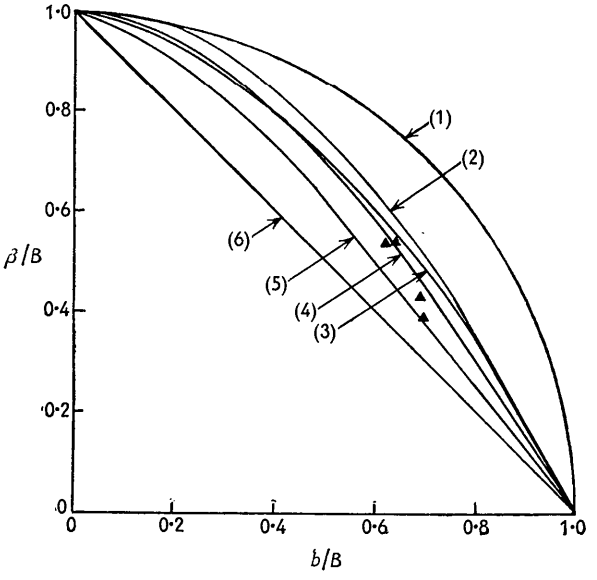

Fig. 3. Relations between β_x, B_x and b_x.
Curve 1: $\beta/B = (1-b^2/B^2)^{\frac{1}{2}}$ (Warren, 1941).
Curve 2: Equation (10) of text.
Curve 3: Relation given by Schoening *et al.* (1952).
Curve 4: Relation given by Alexander & Klug (1950).
Curve 5: Relation given by Jones (1938) and equation (9) of text. These are indistinguishable on the scale used.
Curve 6: $\beta/B = 1-b/B$ (Scherrer, 1920).
Points marked ▲ were obtained by Stokes' method.

almost identical with that of Jones (1938) over the whole range of values, although quite different assumptions were used in the derivations. The curve given by Schoening *et al.* is very similar to one derived for counter diffractometers by Alexander & Klug (1950), although, once again, the assumptions were different. Fig. 3 also shows that these last two curves can be approximated quite closely by the very simple empirical equation

$$\beta_x/B_x = 1-b_x^2/B_x^2 . \qquad (10)$$

Some results obtained by the Stokes method are also included in the figure, but these are inconclusive in indicating the best relation. Attempts were made to test the relations by photographing the same specimen in different cameras and with different radiations, thus varying b_x considerably, and comparing the consistency of the α values. Of course a direct comparison of β_x values would have been preferable, but variation of $b(x)$ also involves variation of x_B (i.e. of ν), so that there is an apparent change of diffraction breadth which can only be eliminated by calculating α. Owing to asymmetry in the geometrical conditions, there is often a discrepancy between the β_x values obtained from the same line on the two sides of one film (this is shown also by Edwards & Lipson's results), so that calculations should be made for each side separately. The results in Table 2 were obtained from

Table 2. *Results for α obtained from the $\{10\bar{1}1\}$ line of one specimen using different radiations and cameras*

Curve of Fig. 3 used for β_x and x_β	Mean value of α	Mean deviation
1	0·149	0·021
2	0·107	0·004
3, 4	0·101	0·006
5	0·087	0·005
6	0·066	0·003

the $\{10\bar{1}1\}$ line in four different photographs, using nickel, cobalt and molybdenum radiations and 9 and 19 cm. diameter cameras.

Obviously Warren's equation is unsatisfactory, and the Fourier results show in any case that curves (1) and (6) are unsuitable. The results do not, however, distinguish between curves (2)–(5) on the basis of consistency, although the values of α obtained from these curves cover a range of 20%. Before considering this question further, we describe how the results in Table 2 are derived. The appropriate relation having been used to calculate β_x, the breadth $\beta_{(\nu)}$ is given by

$$\beta_{(\nu)} = \frac{c^2 \sin 2\theta}{R\lambda^2 L}\beta_x , \qquad (11)$$

where R is the camera radius, λ the X-ray wavelength, θ the Bragg angle of the reflexion, and L the value of h_3 at the peak. This equation is a good approximation and calculation shows that the errors it introduces may be neglected. These errors are greatest for $L = 0$, where the equation predicts $\beta_x = 0$, although this is not strictly true.

Edwards & Lipson (1942) apparently measured the length, x_B, from the peak to one end of the background level in the photometric record, and used equation (11) to calculate ν, replacing β_x by x_B and $\beta_{(\nu)}$ by ν. This procedure neglects the fact that a finite range of x is required to obtain the intensity contained in an infinitesimal range of ξ, as shown by the instrumental broadening of normal lines. The difficulty was mentioned earlier and arises because we are really not able to measure $\beta_{(\nu)}$ for a definite range $\nu = \pm\xi$. However, it is clear that a better approximation is obtained if we assume that ν of equation (8) is related to a quantity x_β which is determined both by x_B and by x_b, the corresponding photometered range for a standard line. The relation between x_β, x_B and x_b is unknown, of course, but must fall within the limits of the possible relations between the breadths, given in Fig. 3. As a purely arbitrary assumption, we have taken the relation to be identical with the breadth relation, so that the curves in Fig. 3 were also used in calculating x_β and hence ν. Equation (8) could then be used to obtain ϱ from $\beta_{(\nu)}$ and ν; to facilitate the calculation of results when growth faulting only had to be considered we plotted curves of α against $\beta_{(\nu)}$ for various values of ν for both odd and even lines. The value of α is actually insensitive to small changes in the value of ν, except when ν is small, so that any correction to x_B of about the right magnitude is satisfactory. It is, however, necessary to make the correction, and the consistency of the results in Table 2 disappears if x_B instead of x_β is used to calculate ν.

A further demonstration of the effects of this correction is given in Table 3. This gives results obtained

Table 3. *The frequency of faults calculated from one line at different arbitrary background levels*

Level	β_x (mm.)	α(using x_B for ν)	α(using x_β for ν)
Measured background	0·415	0·088	0·089
1	0·368	0·082	0·087
2	0·326	0·074	0·090
3	0·282	0·066	0·095
4	0·230	0·057	0·094
5	0·190	0·048	0·086
6	0·127	0·030	0·090

from an experimental $\{10\bar{1}1\}$ line and its neighbouring sharp $\{200\}$ line by assuming various arbitrary background levels above the measured background. The results may be only approximate, because the relation between β_x, b_x and B_x necessarily changes when the background and hence the shapes are materially altered. Nevertheless, the α values obtained by using equation (10) for β_x and calculating ν from x_B clearly show a systematic trend, with the errors due to overestimation of ν becoming important at low ν. The corresponding results obtained when ν is calculated

from x_β are very consistent. The errors in estimation of ν become important for $\nu < 0{\cdot}1$, and in Table 3 this occurs at level 2 (background 8% high). Thus the correction is quite unimportant for the $\{10\bar{1}1\}$ line, but may be appreciable for higher-angle lines, where the photometered range corresponds to smaller values of ν.

The method of using artificial background levels was also used to compare the α values obtained with the use of curves (2)–(5) of Fig. 3. The values obtained at different imaginary levels were most consistent for the group of curves (2)–(4). Using the same experimental line and assumed background levels, values of α were also calculated from $T_{(\nu)}$ and ν, using equation (7). In this case, values of $T_{(\nu)}/T$ could not be determined directly, but a value of T was chosen to give best internal consistency. The results for α, though only approximate, satisfactorily confirmed those from breadth measurements. As a typical example, the mean values of α obtained by breadth measurements with curve (2) of Fig. 3 and by intensity measurements were 0·090 and 0·082, and the mean deviations were 2·8% and 12·9% respectively.

All these results indicate without any certainty that the group of curves (2)–(4) give better results than does curve (5). Since the α values of curves (2)–(4) are almost identical, we have used equation (10) as an adequate representation of them all. The choice is confirmed by comparison of results obtained from $\{10\bar{1}1\}$ lines by the Fourier method and the line-breadth method. In Table 4, this comparison is made

Table 4. *Comparison of values of α obtained by Fourier analysis and line-breadth measurements of $\{10\bar{1}1\}$ lines*

Film No.	α (Fourier analysis)	α (line breadth)
4	0·080	0·063
5	0·082	0·090
6	0·092	0·090
7	0·088	0·102
8	0·085	0·080
36	0·109	0·104
50*	0·051	0·051

* Deformation faults.

on the basis of α values for convenience, but it should be remembered that in each case the quantity actually determined is ϱ. Thus some of the values are fictitious in the sense that deformation faults are also present. Comparison of α values, calculated on the basis of growth faults only, provides a more sensitive indication of the accuracy, since a small change in ϱ produces a relatively large change in α. The agreement may be regarded as satisfactory, and gives reasonable confidence in both methods.

6. The possible occurrence of clustered faults

If line broadening is caused entirely by faulting of one type, a value of α may be obtained from each broadened line of the powder photograph, and the consistency of these values provides the most obvious check on the accuracy of the method. Wilson's calculations (1942), using the experimental data of Edwards & Lipson, gave very consistent results when the correction for photometering range was applied. The actual agreement, however, was obtained only by using average β_x values from both sides of the film, and this is probably not justified, since the individual values for a given line differed by up to 30%.

In some of our films the results for α from different lines were consistent when the method of calculation outlined above was used; in others some differences were found. A typical set of results of the second kind was given by the film analysed by the Fourier method in Fig. 1(*b*) and (*c*), and is shown in Table 5. The

Table 5. *Values of α obtained from a single Debye–Scherrer photograph of cobalt*

Line	2θ (°)	α (random growth faulting)	α (assuming 15% unfaulted)
$\{10\bar{1}1\}$	51·2	0·063	0·078
$\{10\bar{1}2\}$	67·8	0·044	0·076
$\{10\bar{1}3\}$	92·0	0·050	0·076
$\{20\bar{2}1\}$	104·3	0·063	0·076
$\{20\bar{2}2\}$	119·7	0·055	0·090
$\{20\bar{2}3\}$	155·3	0·055	0·074

$\{10\bar{1}4\}$ line too faint for reliable measurements.

lower values of α from the even lines suggest that the faulting is of mixed type, and we have seen that this satisfactorily explains the Fourier results. The alternative assumption of an unfaulted fraction has also been mentioned, and in the last column of the table we show the improvement thus obtained. Similar improvements were found to be possible in all the inconsistent films by this method, so that the model may be justified.

In specimens containing either growth or deformation faults alone, calculations indicated that the most consistent results were obtained by using curve (2) of Fig. 3, rather than curve (5).

7. Conclusion

The measurement of both α and α' requires the determination of ϱ_o and ϱ_e from two lines of the powder photographs. Our results indicate that a reliable value of ϱ_o may be obtained from the $\{10\bar{1}1\}$ line by the Fourier method, and a less reliable value of ϱ_e from the $\{10\bar{1}2\}$ line. Line-breadth measurements give satisfactory results in most circumstances, and are particularly valuable in deciding whether the faulting is predominantly of one type. Spontaneously transformed cobalt specimens often contain predominantly growth faults, whereas specimens which have been stressed to complete the transformation contain deformation faults. Specimens with mixed faulting have also been encountered, and although

line-breadth measurements indicate that these results can also be explained as a clustering of the growth faults, this is not supported by the Fourier data.

Financial support for the experimental work was obtained from a grant made to this laboratory for general research purposes by the British Non-Ferrous Metals Research Association, and also from the Rhodes Trustees, Oxford. We should like to thank Dr W. Hume-Rothery for his interest.

APPENDIX

We derive the relation between B_x, b_x and β_x when $b(x) = c/(1+k^2x^2)^2$ and $\beta(x)$ is determined by equation (1). If the cosine Fourier transforms of $B(x)$, $b(x)$ and $\beta(x)$ are $L(t)$, $M(t)$ and $N(t)$, it follows from equation (5) that

$$L(t) = (2\pi)^{\frac{1}{2}}M(t)N(t) .$$

From the assumption about $b(x)$,

$$M(t) = (\pi/2)^{\frac{1}{2}}(c/2k)(1+t/k)\exp(-t/k) .$$

Since x is very nearly a linear function of ξ over the range of interest, we may measure x in units of ξ and write equation (1) in the form

$$\begin{aligned}\beta(x) &= C[1+2\sum_1^\infty \varrho^m \cos \pi m x] \\ &\cong 2C\int_0^\infty \varrho^m \cos \pi m x\, dm \\ &= \frac{2C}{\pi}\int_0^\infty \varrho^{t/\pi}\cos xt\, dt ,\end{aligned}$$

where $t = \pi m$. The Fourier transform is thus

$$N(t) = (\pi/2)^{\frac{1}{2}}(2C/\pi)\varrho^{t/\pi} .$$

In order to proceed further, we have to use the approximate expression, valid for small α,

$$\varrho = \exp(-\beta_x) ,$$

and we also have $b_x = \pi/2k$. We thus obtain

$$L(t) = A(1+2b_xt/\pi)\exp\{-(2b_x+\beta_x)t/\pi\} ,$$

where A is a constant.

The breadth B_x is given by

$$B_x = 2\int_0^\infty B(x)dx/B(0) = \pi L(0)\Big/\int_0^\infty L(t)dt .$$

Since $L(0) = A$ and

$$\int_0^\infty L(t)dt = A\left[\frac{\pi}{2b_x+\beta_x}+\frac{2\pi b_x}{(2b_x+\beta_x)^2}\right] ,$$

we find

$$B_x = (2b_x+\beta_x)^2/(4b_x+\beta_x) .$$

The solution of this equation gives equation (9).

References

Alexander, L. & Klug, H. P. (1950). *J. Appl. Phys.* **21**, 137.

Anantharaman, T. R. & Christian, J. W. (1953). *Brit. J. Appl. Phys.* **4**, 155.

Christian, J. W. (1954). *Acta Cryst.* **7**, 415.

Eastabrook, J. N. & Wilson, A. J. C. (1952). *Proc. Phys. Soc.* B, **65**, 67.

Edwards, O. S. & Lipson, H. (1942). *Proc. Roy. Soc.* A, **180**, 268.

Frank, F. C. & Nicholas, J. F. (1953). *Phil. Mag.* (8), **44**, 1213.

Gevers, R. (1953). *Natuurwet. Tijdschr.* **35**, 25.

Gevers, R. (1954). *Acta Cryst.* **7**, 337.

Jagodzinski, H. (1949). *Acta Cryst.* **2**, 201.

Jones, F. W. (1938). *Proc. Roy. Soc.* A, **166**, 16.

Paterson, M. S. (1952). *J. Appl. Phys.* **23**, 805.

Rachinger, W. A. (1948). *J. Sci. Instrum.* **25**, 254.

Scherrer, P. (1920). *Kolloidchemie*, 3rd edition, p. 387. Leipzig: Spamer.

Schoening, F. R. L., Niekerk, J. N. van, & Haul, R. A. W. (1952). *Proc. Phys. Soc.* B, **65**, 528.

Stokes, A. R. (1948). *Proc. Phys. Soc.* **61**, 382.

Warren, B. E. (1941). *J. Appl. Phys.* **12**, 375.

Williamson, G. K. & Smallman, R. E. (1954). *Acta Cryst.* **7**, 574.

Wilson, A. J. C. (1942). *Proc. Roy. Soc.* A, **180**, 277.

Wilson, A. J. C. (1949). *X-Ray Optics*. London: Methuen.